

Ionospheric Scintillation Morphological Analysis Using GPS-SCINDA Data at Low Latitude Ground Station

Mohammed Ayalew Belay¹

¹Hawassa University

November 24, 2022

Abstract

This study aims to present the morphology of GPS L-band scintillations at the equatorial anomaly station Bahir Dar (11030'N, 37030'E) using GPS-SCINDA data in the descending high solar activity period between January 2014 to December 2014. In studying low-latitude scintillation, we have used millions of data recorded every minute of one year by 32 GPS satellite and it is found that intense scintillation occurred during the day time with a small frequency and very frequent occurrences of relatively moderate scintillation during the night time. In the period of observation, the variation of scintillations with local time and season are analyzed and it is found that occurrence of scintillation is minimum in summer months and maximum in equinox months with highest values observed in the months of March and September. Pre-midnight and post-midnight occurrence of scintillation is also studied and Pre-midnight scintillation was found to be maximum in equinox whereas it is minimum in winter months. Generally, it is found that most of scintillations are weak ($s_4 < 0.1$) and intense scintillations with $s_4 > 0.3$ are rare.

1 **Ionospheric Scintillation Morphological Analysis Using GPS-SCINDA Data at Low**
2 **Latitude Ground Station**

3 **M. Ayalew¹**

4 ¹Hawassa University.

5 Corresponding author: Mohammed Ayalew(zeru326@gmail.com)

6 **Key Points:**

- 7 • At our location we have frequent occurrence of weak ionospheric scintillations, while
8 few intense scintillations.
- 9 • Intense scintillation occurred during the day time with a small frequency and relatively
10 moderate scintillation occurrence during the night time with very frequent occurrence of
11 scintillation.
- 12 • The maximum numbers of amplitude scintillation events are observed in equinox and
13 minimum in summer.
- 14 • In summer, winter and equinox, high scintillations occurred at 19:00:00, 21:00:00 and
15 22:00:00 in pre-midnight local time hours respectively, while at in post mid-night period
16 it is 04:00:00, 00:00:00 and 01:00:00 local time hours respectively.
17

18 **Abstract**

19 *This study aims to present the morphology of GPS L-band scintillations at the equatorial*
20 *anomaly station Bahir Dar (11030'N, 37030'E) using GPS-SCINDA data in the descending high*
21 *solar activity period between January 2014 to December 2014. In studying low-latitude*
22 *scintillation, we have used millions of data recorded every minute of one year by 32 GPS*
23 *satellite and it is found that intense scintillation occurred during the day time with a small*
24 *frequency and very frequent occurrences of relatively moderate scintillation during the night*
25 *time. In the period of observation, the variation of scintillations with local time and season are*
26 *analyzed and it is found that occurrence of scintillation is minimum in summer months and*
27 *maximum in equinox months with highest values observed in the months of March and*
28 *September. Pre-midnight and post-midnight occurrence of scintillation is also studied and Pre-*
29 *midnight scintillation was found to be maximum in equinox whereas it is minimum in winter*
30 *months. Generally, it is found that most of scintillations are weak ($s_4 < 0.1$) and intense*
31 *scintillations with $s_4 > 0.3$ are rare.*

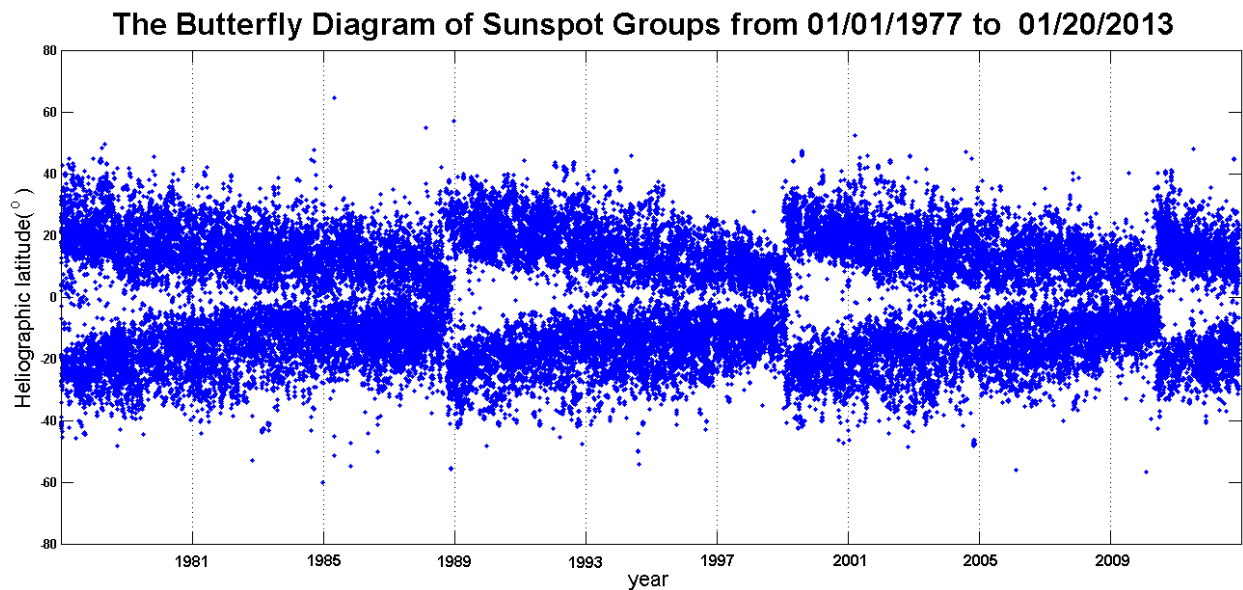
32

33 **INTRODUCTION**

34

35 The ionosphere is a partially ionized part of the upper atmosphere where free electrons are
36 concentrated and affect the propagation of GPS radio frequency electromagnetic waves. The
37 ionosphere owes its existence to the sun through photoionization. The Sun continuously emits
38 energy into space in the form of electromagnetic (EM) radiation and energetic particles in what
39 is called solar wind. The solar wind, which expands out into the Solar System carrying with it
40 the Sun's magnetic field, carves out a region of interplanetary space called the heliosphere and
41 forms the interplanetary magnetic field. The solar wind and EM radiation is not steady due to
42 the dynamic processes in the sun. Among the most prominent indicators of its evolving, non-
43 static nature of sun are sunspots. Sunspots appear as dark areas on the solar surface and have
44 been observed to peak in number approximately every 11 years [1]. The natural differential
45 rotation of the sun triggers sunspots to collide and causes violent eruption of radiation and
46 matter, solar flare and coronal mass ejection (CME) respectively, in a period of approximately
47 eleven years, known as the solar cycle shown in figure 1. The ejection of sudden CME causes a
48 disturbance in the interplanetary magnetic field and initiates a disturbance on the geomagnetic
49 field, known as the geomagnetic storm. Due to the interaction of geomagnetic field with the
50 ionospheric plasma, geomagnetic storm triggers electron density irregularities. Thus, electron
51 production and irregularities in the ionosphere is controlled by ionization processes that

52 primarily depend on a wide spectrum of solar X-ray and extreme ultraviolet (EUV) radiation
 53 which varies with the Sun's activity. Without the solar activity, the ionosphere would possess a
 54 reasonably deterministic variability, which is associated with the local solar zenith angle,
 55 including diurnal and seasonal effects that are appreciably controlled by geometry. Therefore,
 56 ionospheric electron density depends on time (diurnal and seasonal), geographical location
 57 (polar, auroral zones, mid latitudes, and equatorial regions), and with certain solar related
 58 ionospheric instabilities. These changes affect Earth's space environment in a number of ways,
 59 including increased solar wind that bombards Earth's upper atmosphere, causing aurorae and
 60 large electrical currents that can disrupt communication, power grids, and satellite navigation
 61 including the GPS system.



63 Figure 1: The butterfly diagram of sunspot groups.

64 One of the first known effects of space weather on GPS was fluctuations in the amplitude and
 65 phase of GPS radio signals known as ionospheric scintillation. Ionospheric scintillation is a
 66 rapid and irregular fluctuations of amplitude and phase of radio wave transmissions from
 67 satellites received at the earth surface resulting from electron density irregularities in the
 68 ionosphere [2]. The fluctuations in electron density cause perturbations in the index of
 69 refraction of the ionosphere, which in turn cause diffraction of the radio waves. Multiple
 70 diffracted wave fronts, with different phases, reach the antenna receiver at the same time.
 71 Because the ionospheric irregularities causing the diffraction as well as the GPS satellites are

72 moving, the receiver experiences alternating periods of constructive or destructive signal
73 interference, and fluctuations in the phase and amplitude of the received signal develop.

74 Although scintillation can occur anywhere over the Earth, globally there are two zones of
75 severely affected by scintillation activity, one in the equatorial zone which extends up to $\pm 20^\circ$
76 in geomagnetic latitude around the magnetic equator forming a scintillation belt that
77 encompasses approximately 1/3 of the Earth's surface and another at high latitudes in the
78 vicinity of auroral to polar latitude. In the equatorial zone, enhanced scintillation activity has
79 been observed in the equatorial ionization anomaly (EIA) belt ($10\text{--}20^\circ$ lat. on either side of the
80 magnetic equator) as compared to that at nearby low latitudes. This region is highly dynamical,
81 unpredictable and is characterized by the existence of intense plasma irregularities which affect
82 almost all radio communication systems utilizing the earth space propagation path. Ionospheric
83 scintillations, the most significant manifestation of ionospheric irregularities, poses a challenge
84 to GPS users, satellite communications, and radar system performance and radio astronomical
85 observations [3]. Ionospheric scintillation will degrade the GPS signal quality, reduce its
86 information content, or cause failure of the GPS signal reception and under the worst of
87 conditions, it can lead to communication blackouts [4]. With the increasing applications of
88 Global Positioning Systems (GPS) and satellite-based communication and navigational
89 systems, especially when the millimeter range precision approach is required, the precise
90 occurrence characteristics and prediction of the intensity of scintillations and their effects on L-
91 band frequencies is important.

92

93 RELATED WORKS

94

95 Extensive studies of GPS ionospheric scintillations have been carried out over the past four
96 decades in different parts of the world under national and international space weather science
97 research programs. A number of reviews articles covering different aspects and features of
98 ionospheric scintillations and ionospheric irregularity mechanisms based on theoretical and
99 experimental observations have been published. These studies indicated that scintillations
100 phenomenon have strong diurnal, seasonal, geographic and solar cycle dependence being at

101 their most severe during the evening hours, in the months of the equinox, at equatorial latitudes
102 and during the years of solar maximum.

103 As the ionosphere over Ethiopia is situated in one of the highly dynamic regions of the world,
104 covering the geomagnetic equator to the ionization anomaly crest region and beyond, a GPS
105 scintillation network decision aid (GPS-SCINDA) station was established at Bahir Dar with
106 help of US Air Force to study the temporal, seasonal, solar activity variations of scintillations.
107 In this study, we have investigated GPS scintillations from data collected at the equatorial
108 anomaly station Bahir Dar for the descending high solar activity period 2014-2015. During the
109 observation period, scintillation parameters were extracted from dual frequency GPS receiver
110 installed at Bahir Dar.

111 DATA AND METHODOLOGY

112 EXPERIMENTAL SETUP

113

114 When the irregular electron content of the ionosphere drift across the path of the GPS signal,
115 the spatial pattern of varying intensity is converted into temporal fluctuations or scintillations
116 and recorded by GPS ionospheric scintillation and TEC monitoring (GISTM) ground receiver.
117 The scintillation data used in this study originates from GISTM measurement using high data-
118 rate Novatel GSV400B GPS SCINDA dual frequency (L1=1575.42 MHz and L2=1227.60
119 MHz) receiver situated at Bahir Dar University, Bahir Dar, Ethiopia (lat. 23.2° N, long.77.6° E)
120 near the northern crest of the equatorial anomaly. The site located near the crest of the
121 equatorial ionization anomaly and therefore well situated for the measurement of TEC and
122 Ionospheric scintillation. This has been the drive for the commencement of ionospheric
123 measurement equipment (GPS-SCINDA System) by Boston College in collaboration with the
124 Air Force Research Laboratory (AFRL) over Ethiopia for such studies.

125 THE GPS-SCINDA SYSTEM

126

127 The Scintillation Network and Decision Aid (SCINDA) is a network of ground-based receivers
128 that monitors scintillations at the UHF and L-band frequencies caused by electron density
129 irregularities in the equatorial ionosphere [5]. SCINDA was developed to provide short-term
130 forecasts of scintillation to operational users in real time. The SCINDA ground stations are
131 generally positioned between the ionization crests of the Appleton anomaly, as these locations
132 experience the strongest global levels of scintillation. The SCINDA network supported by a
133 modular and portable software called GPS-SCINDA. The GPS SCINDA is a real-time GPS
134 data acquisition and ionospheric analysis software, written in C for the LINUX operating
135 system. GPS-SCINDA was also developed for Air Force Space Command by the AFRL's
136 Ionospheric Hazards Branch to predict communication satellite outages in the equatorial region
137 that are caused by naturally-occurring disruptions in the ionosphere. The software provides
138 measurements of S4, TEC, and ROTI (rate of change of TEC), as well as receiver position in
139 real time using the full temporal resolution of the receiver hardware. GPS-SCINDA measures
140 the scintillation intensity index on both the L1 and L2 signals. The GPS-SCINDA system
141 consists of a GPS receiver, a GPS antenna, the GPS-SCINDA data collection software and a
142 computer running the LINUX operating system with access to the Internet [6]. In this study, the
143 analysis of the scintillation and TEC data has been carried out using the GPS TEC analysis
144 application software called WinTEC-P, which was developed by Carrano and Groves (2009) at
145 the Institute of Scientific Research, Boston College, USA. WinTEC-P utilizes the GPS-
146 SCINDA ionospheric statistics file (*.scn) and the position file (*.psn) to obtain coordinates of
147 the station, if it is not specified in its configuration. The software includes an algorithm for the
148 estimation and removal of instrumental biases associated with the GPS receiver and the GPS
149 satellites. The biases free TEC (Vertical TEC) and s4 index are written in ASCII output files
150 together with other parameters defining the position of the satellite such as the time, elevation
151 angle, azimuth angle, and the longitude and latitude of the Ionospheric Pierce Points (IPP). It
152 also includes programs written in the GNU R to plot S4 and calibrated TEC and Perl Scripts to
153 automatically generate and archive daily S4 and TEC plots with 15-minute updates.

154 The fluctuations in the signal intensity or severity of amplitude scintillation is measured by the
155 scintillation intensity index S4 which is defined as the normalized variance of the signal power
156 [7].

$$S_4 = \sqrt{\frac{\langle I^2 \rangle - \langle I \rangle^2}{\langle I \rangle^2}}$$

157 Where I is the signal intensity (amplitude squared) averaged for 60 seconds.

158 METHOD OF ANALYSIS

159

160 For this study the scintillation occurrence of the data collected at equatorial anomaly station
 161 Bahir Dar are examined throughout the descending high solar activity period of January 2010 to
 162 December 2010 by dividing it into three seasons, E-months (March, April, September, October)
 163 D-months (November, December, January, February), J-months (May, June, July, August). The
 164 estimations were also limited to measurements made from satellites with elevation angle higher
 165 than 30^0 . GPS scintillation occurrence is investigated separately in hour, month, and seasonal
 166 variation. In order to study the level of scintillation we have chosen four distinct thresholds
 167 which are named as weak, moderate, strong and saturated as given by Gwal et al., (2004) shown
 168 in table 1.

Thresholds	S4 index
weak	$0.2 < S_4 \leq 0.4$
moderate	$0.4 < S_4 \leq 0.6$
strong	$0.6 < S_4 \leq 1.0$
saturated	$1.0 < S_4 \leq 1.4$

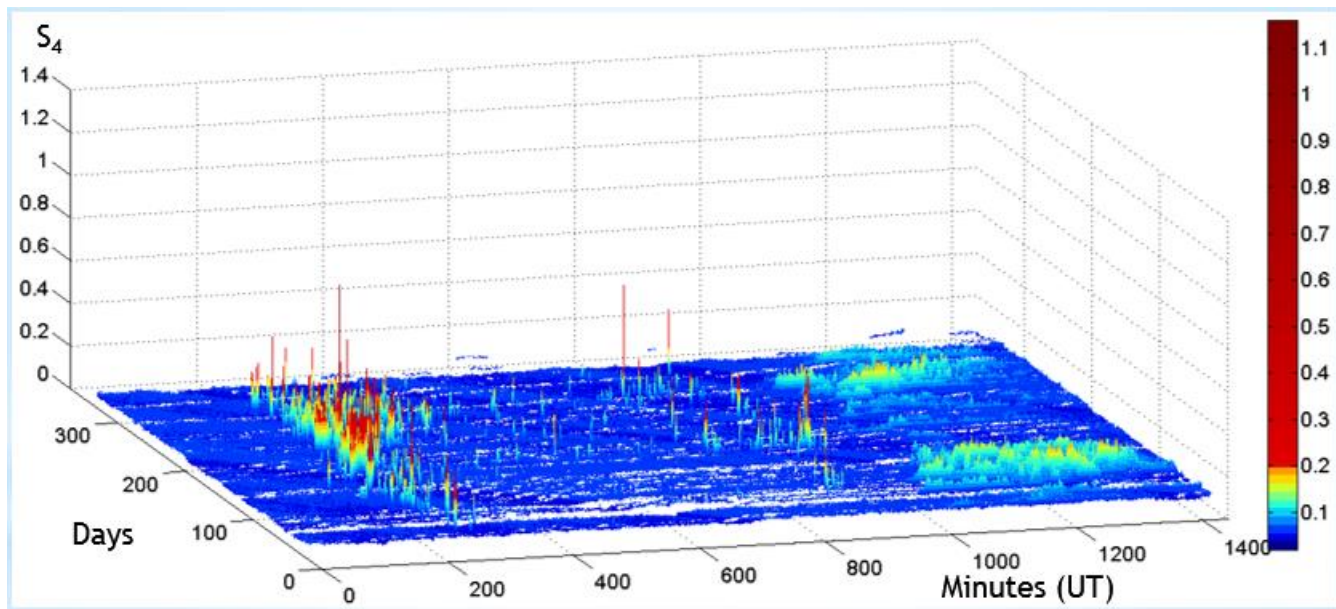
169

Table 1: level of scintillation

170 RESULT AND DISCUSSION

171

172 Ionospheric scintillation index and total electron characteristics are plotted by using more than
 173 five million raw data from 32 satellites. Figure 3 presents the diurnal variation of S4 from
 174 January to December 2014. The general trend shown by the surface plots indicate that the S4
 175 value range from 0.02 to 1.14. Particularly, the smallest values are observed from 0200 to 2000
 176 in almost the cases. The relatively high values are observed from 2000 to 0200 and ranged from
 177 0.08 to 0.14. This general trend confirms the fact that the scintillation is significant during the
 178 night. However, it can be seen from figure three that small amount of intense scintillation
 179 occurred during the day time. The result generally exhibits an occurrence frequency of
 180 scintillation observed mainly at nighttime hours (2000-0000 extended to 0200 LT in some



181 cases).

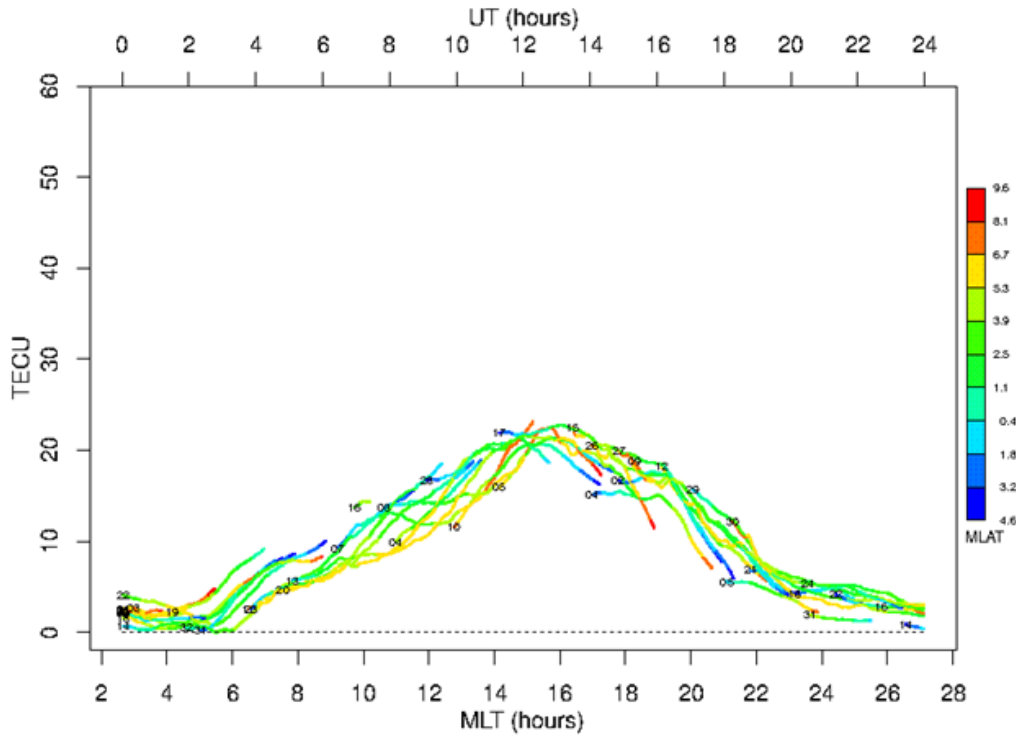
182

183 Figure 3: Diurnal variation of S4 from January to December 2014

184

185 A typical representation of the variation of the TEC for the period under consideration is shown
 186 in figure 4. The legend in the figures shows the graduation of the geomagnetic Latitude
 187 (MLAT) of the satellite pass. The TEC follows a three-segment process as expected in a low-
 188 latitude station. At the beginning TEC attains a value of zero about 04:00 UT and quickly
 189 increases to reach a maximum value of 25 TECu at about noon forming a plateau, which is a

190 comparatively stable region for about three hours before going to the decay region with a value
 191 of 3 TECu at 22:00 UT.



192

193

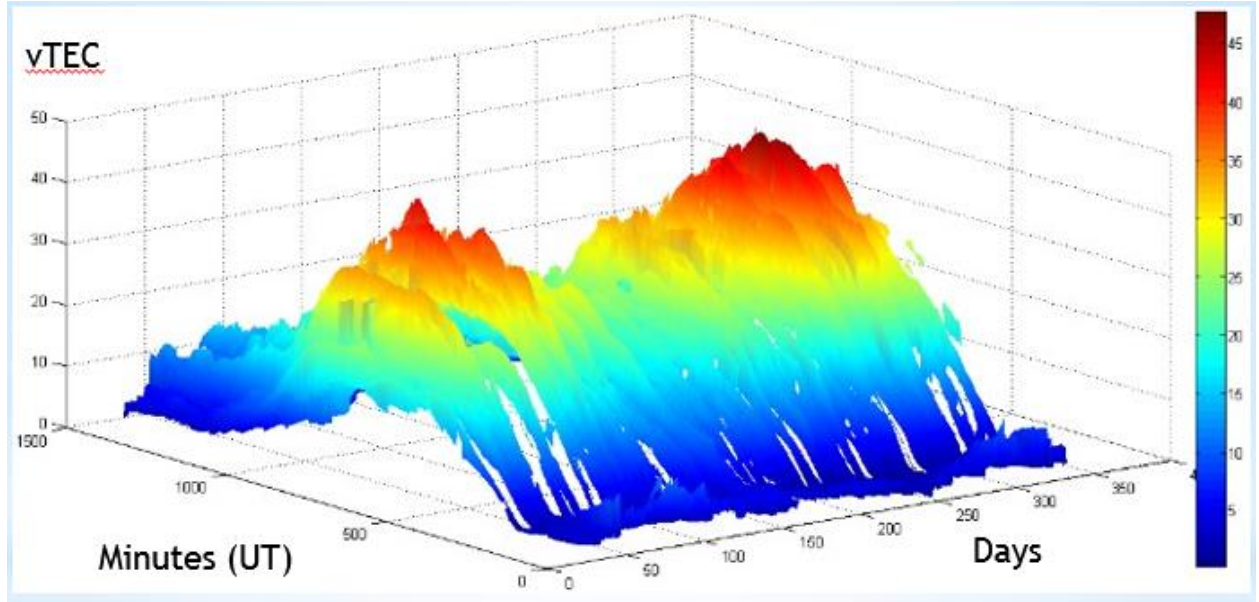
Figure 4. Typical diurnal variation of VTEC

194 The diurnal variation of VTEC from January to December 2014 is presented in figure 5a & b.

195 The surface plot indicates that the minimum value is near sunrise, then TEC increase until

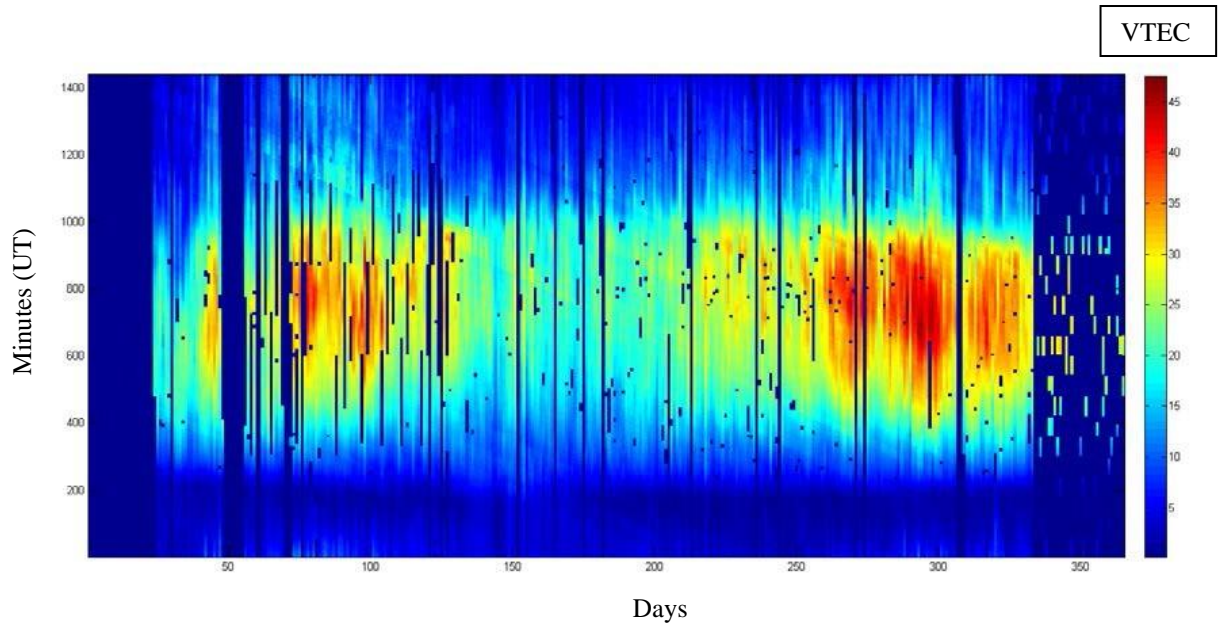
196 maximum value is around 1400-1500 L T, after that decrease through the night. It also indicates

197 that the VTEC value range from 5 to 45.



198

199 Figure 5a: Diurnal variation of VTEC shown in 3D plot from January to December 2014

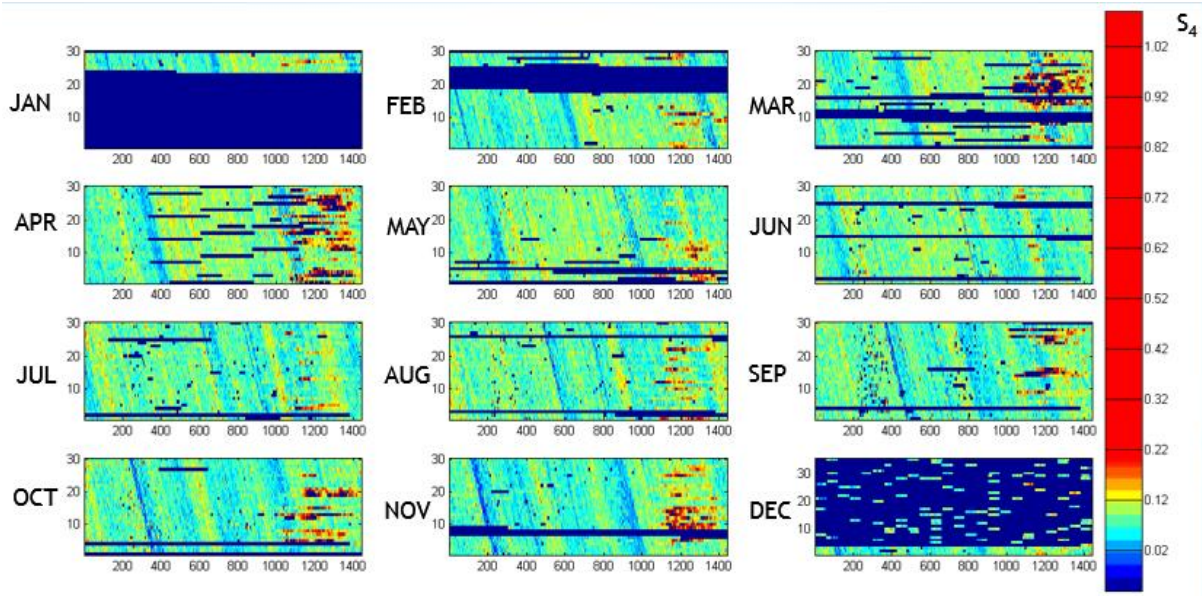


200 Figure 5b: Variation of VTEC in the year 2014

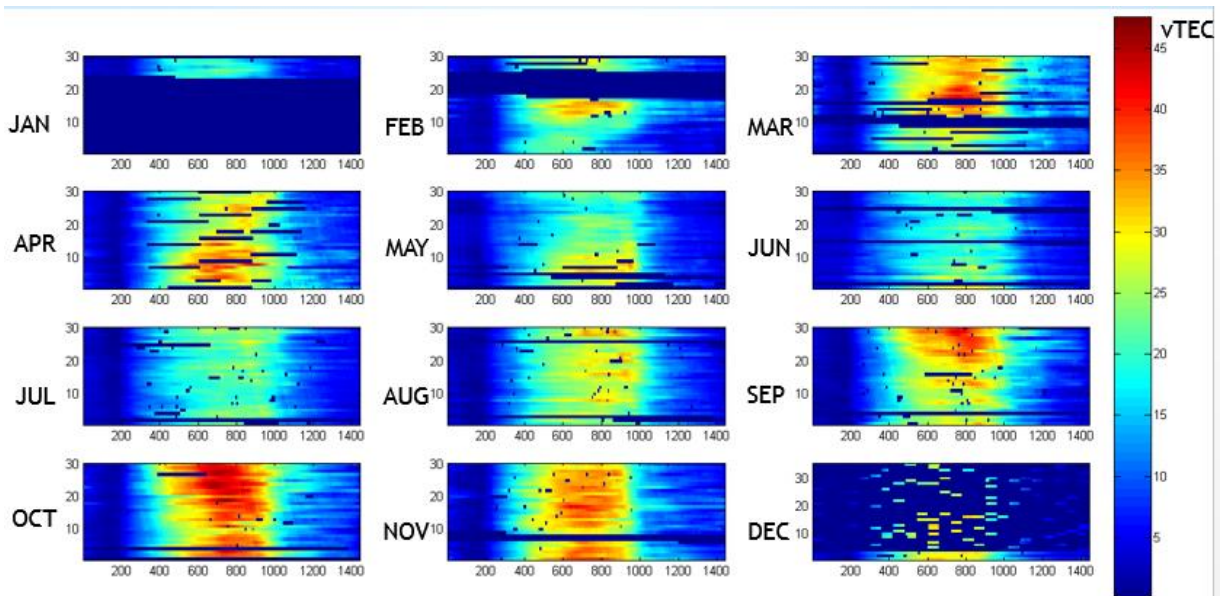
201 The monthly variation of the scintillation index S4 is shown in figure 6. In all the plots, larger
202 proportion of the data lies below 0.1, and sparsely distributed at higher values. At unity and
203 beyond, the data were extremely rare, even during active periods of scintillations. March, April,
204 February, September–December recorded scintillation events at moderate and intense levels,

205 and these events were generally localized within 1930LT–2400LT, although, the distributions
206 were observed to extend to around 0300LT during January, February and December. All other
207 months experienced weak scintillation of various degrees of occurrences.

208



209



210 Figure 6: Monthly variation of the scintillation index S_4

211 Figure 7: Monthly variation of the vTEC

212 Separately for each month, the result for the vTEC is presented in figure 7. The diurnal
213 variation shows that vTEC variation depends on the solar zenithal angle. vTEC values are lower
214 than 20 TECU from midnight to 1100 and from 1700 to midnight. The highest values of vTEC
215 are spotted during the day and particularly around 1500 LT where we have values greater than
216 20 TECU. The highest values are observed in the months of March, October and September.

217 CONCLUSION AND FUTURE WORK

218 Based on the analyzed amplitude scintillation GPS-SCINDA data for year 2014, the following
219 conclusions can be drawn.

- 220 • At our location we have frequent occurrence of weak ionospheric scintillations, while
221 few intense scintillations.
- 222 • Intense scintillation occurred during the day time with a small frequency and relatively
223 moderate scintillation occurrence during the night time with very frequent occurrence of
224 scintillation.
- 225 • The maximum numbers of amplitude scintillation events are observed in equinox and
226 minimum in summer.
- 227 • In summer, winter and equinox, high scintillations occurred at 19:00:00, 21:00:00 and
228 22:00:00 in pre-midnight local time hours respectively, while at in post mid-night period
229 it is 04:00:00, 00:00:00 and 01:00:00 local time hours respectively.

230 REFERENCE

- 231
- 232 [1] G. Prölss, *Physics of the Earth's Space Environment: An Introduction*. 2004.
 - 233 [2] E. J. Liberman, "HOLES: IONOSPHERIC SCINTILLATION GPS AND
234 IMPUTATION," no. March, 2015.
 - 235 [3] A. W. Wernik, J. A. Secan, and E. J. Fremouw, "Ionospheric irregularities and
236 scintillation," *Adv. Sp. Res.*, vol. 31, no. 4, pp. 971–981, 2003.
 - 237 [4] T. C. Miller and R. J. Sullivan, "Ionospheric Scintillation Effects on a Space-Based ,
238 Foliage Penetration , Ground Moving Target Indication Radar," no. August, 2001.
 - 239 [5] C. S. Carrano and K. M. Groves, "The GPS segment of the AFRL-SCINDA global
240 network and the challenges of real-time TEC estimation in the equatorial ionosphere,"

- 241 *Proc. Inst. Navig. Natl. Tech. Meet.*, vol. 2, no. January, pp. 1036–1047, 2006.
- 242 [6] C. S. Carrano, “GPS - SCINDA : A Real - Time Gps Data Acquisition and Ionospheric
243 Analysis System for Scinda,” no. X, pp. 1–62, 2007.
- 244 [7] X. Pi, A. J. Mannucci, and A. Freeman, “Global Distribution of L-Band Ionospheric
245 Scintillation,” pp. 1–4, 2011.
- 246